



## Copper (II) oxide thin film for methanol and ethanol sensing

Mitesh Parmar and K.Rajanna

Department of Instrumentation and Applied Physics,

Indian Institute of Science,

Bangalore- 560012, India

Emails: [mitesh.iisc@gmail.com](mailto:mitesh.iisc@gmail.com), [kraj@isu.iisc.ernet.in](mailto:kraj@isu.iisc.ernet.in)

---

*Submitted: Nov. 1, 2011*

*Accepted: Nov. 24, 2011*

*Published: Dec. 6, 2011*

---

*Abstract- A nanostructured copper (II) oxide film deposited by reactive DC-magnetron sputtering technique, has been studied for static sensor response towards methanol and ethanol by operating temperature and analyte concentration modulations. The optimum operating temperature ( $T_{opt}$ ) for the sensing of methanol and ethanol is observed to be 350 °C and 400 °C, respectively. The maximum sensitivity observed for 2500 ppm methanol and ethanol is 29% and 15.4% respectively. Another important observation is that the sensitivity time reduces with analyte concentrations, where as recovery time increases. The response time of 2500 ppm methanol and ethanol is 235 s and 247 s correspondingly.*

**Index term:** Copper (II) Oxide thin films, sputtering, gas sensing, response time and recovery time.

## I. INTRODUCTION

It is interesting to find the new materials and to study the material properties suitable for the various applications, as sometimes that will be a key to overcome many challenges and problems. During 1950s, Brattain *et al.* [1], Heiland [2] and Bielanski *et al.* [3] have initiated the research on gas sensing by observing the effect of ambient gas on the electrical conductivity of the materials. In 1962, further impetus to this was given by Seiyama *et al.* by discovering the change in the electrical conductivity of ZnO thin film by the presence of reactive gases in the air [4]. Since then, various types of sensing materials have been reported in the literature ranging from SnO<sub>2</sub>, ZnO, TiO<sub>2</sub>, WO<sub>3</sub>, In<sub>2</sub>O<sub>3</sub> to CuO, Fe<sub>2</sub>O<sub>3</sub>, NiO, and Y<sub>2</sub>O<sub>3</sub> [5]. Recently, CuO is used to enhance the gas sensor response of common metal oxides such as SnO<sub>2</sub>, ZnO, etc. [6–9]. The suitability of CuO as homogeneous sensing material is one of the ongoing research problem and in this paper we have tried to contribute in the same regard.

Although generally CuO is p-type semiconducting material [5, 10, 11] due to copper vacancies [11], there has been reports of CuO being n-type semiconducting nature [5]. The p-type semiconducting CuO responds differently compared to normal metal oxides such as ZnO, TiO<sub>2</sub>, SnO<sub>2</sub> and WO<sub>3</sub> which are n-type in nature. While observing the advantages of p-type oxides, the temperature dependence of conduction in high-temperature range is considerably less in the p-type oxides than that of n-types [5, 12]. Moreover, p-type oxides have tendency to exchange lattice oxygen easily with air [5, 13]. During lifetime of the sensor, this can be useful in maintaining stoichiometry of the oxides. These advantages in turn can be important to maintain long-term stability of the sensor and improve the lifetime of the sensor, if used tactfully. Considering disadvantages of p-type oxides, the most important is the mobility of their charge carriers which can affect the sensitivity, response and recovery time of the sensor. This disadvantage of p-type oxides can be overcome by varying the film morphology, electrode configuration and using suitable catalyst. The use of CuO as homogeneous sensing film for CO<sub>2</sub> sensing is first reported by Ishihara *et al.* [14]. As CO<sub>2</sub> is one of the by-products during dehydrogenation of alcohols, CuO can be used as alcohol sensing material. In the case of CuO, the material resistance increases (instead of decreasing as in the case of n-type) during the sensing of alcohol.

There have been reports of some interesting work based on this material, for example,

work reported by Wang *et al.* [10]. Although the work about CuO nanorods prepared by hydrothermal method is impressive, and shows very good response for ethanol sensing, the sensing is observed only at 300 °C. Moreover, there is no plausible reason for using 300 °C as operating temperature for the sensor. In addition to this, there are no detailed reports on methanol sensing using CuO thin films.

In our present work, the detailed study is performed on the static sensing behavior of reactively-sputtered nanostructured CuO film for ethanol as well as methanol by modulations of operating temperatures and analyte concentrations. In addition to this, we are presenting the dependency of sensing response time as well as recovery time on the analyte concentration. In order to check the reproducibility and repeatability, all the observations are done for at least 3–5 times, and results are plotted with error-bars. The preliminary work carried out by us in this regard has been reported elsewhere [15].

## II. EXPERIMENTAL

### 2.1. Deposition of the films

The sensor is fabricated with nanostructured CuO as a sensing film, deposited over 1 μm thick SiO<sub>2</sub> coated Si substrate, using reactive DC-magnetron sputtering technique. Silver contact films on either end of the sensing film are deposited in order to get two-end electrode configuration. As the Ag electrodes are fabricated over the sensing films are 6 mm apart, the catalytic activities due to diffusion of Ag into CuO sensing material, can be neglected. In order to avoid the oxidization of Ag during the sensing, 10 nm gold film is used as protecting layer. Fig. 1 shows the schematic diagram of the sensor.

The sensor consists of dc-magnetron sputtered nanostructured CuO sensing film over comb-type silver electrode deposited over 1 μm thick SiO<sub>2</sub> coated Si substrate. The contact films on either end of the sensing film are deposited in order to get two-end electrode configuration. As the Ag electrodes are fabricated over the sensing films are 6 mm apart, the catalytic activities due to diffusion of Ag into CuO sensing material, can be neglected. Fig. 1 shows the schematic diagram of the sensor.

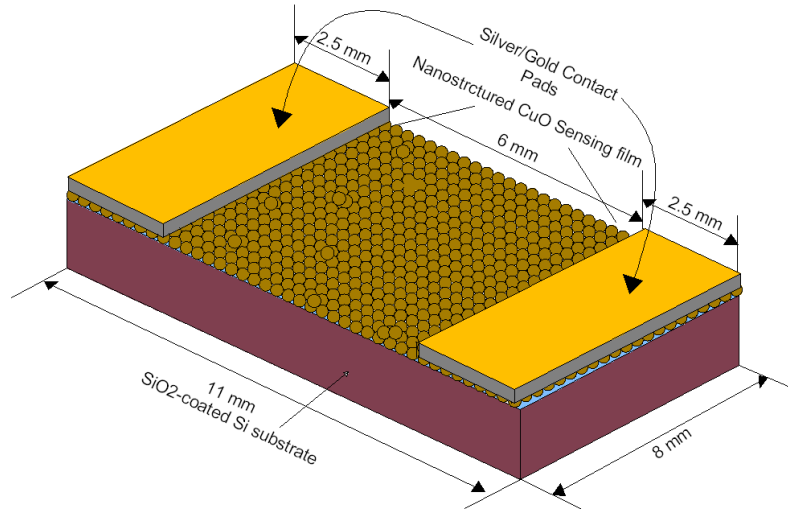


Figure 1. Schematic diagram of the sensor.

The optimized sputtering process parameters for the deposition of Au, Ag and CuO films, using gold, silver and Oxygen Free High Conductive (OFHC) copper target materials, are given in Table 1. Pre-sputtering of these targets is done appropriately for some time, in order to remove the surface impurities. The thicknesses of the films are measured by the surface profilometer – Taylor Hobson - Form Talysurf Plus.

Table 1: Optimized sputtering process parameters for the deposition of CuO, Ag and Au films.

Sputtering Parameter	Materials deposited		
	CuO	Ag	Au
Working distance (mm)	55	55	52
Substrate Temperature (°C)	375	Room Temp.	Room Temp.
Ultimate Vacuum (mbar)	$1 \times 10^{-6}$	$3.7 \times 10^{-6}$	$8 \times 10^{-6}$
Argon-Oxygen Ratio	90:10	NA	NA
Working pressure (mbar)	$3 \times 10^{-2}$	$3.5 \times 10^{-2}$	$8 \times 10^{-3}$
Current density (mA/cm <sup>2</sup> )	0.679	0.51	0.334
Deposition rate (nm/minute)	5.67	18	50
Film thickness (nm)	85	180	≈10

## 2.2. Characterization of the film

The crystal structure of the sensing sample is determined by X-ray diffraction (XRD) using Bruker D8 Advance X-ray diffractometer with Cu  $K_{\alpha}$  radiation of wavelength 1.54 Å. The XRD spectrum is recorded in the range,  $2\theta = 20^{\circ}$ – $50^{\circ}$ . For the XPS analysis, SPECS GmbH spectrometer (Phoibos 100MCD Energy Analyzer) using Mg $K_{\alpha}$  radiation (1253.6 eV) and CASA XPS analysis software is used. The morphologies of the sensing film is investigated using FEI Quanta 200 Environmental scanning electron microscope (ESEM).

## 2.3. Design of experimental set-up to study sensing behaviour and the sensing procedure

The gas sensing measurements is done with the help of in-house designed testing set-up as shown in Fig. 2. The sensor sample is placed over a heater (accuracy  $\pm 1^{\circ}\text{C}$ ) located inside the chamber, and pressure-contacts are used for monitoring electrical behaviour.

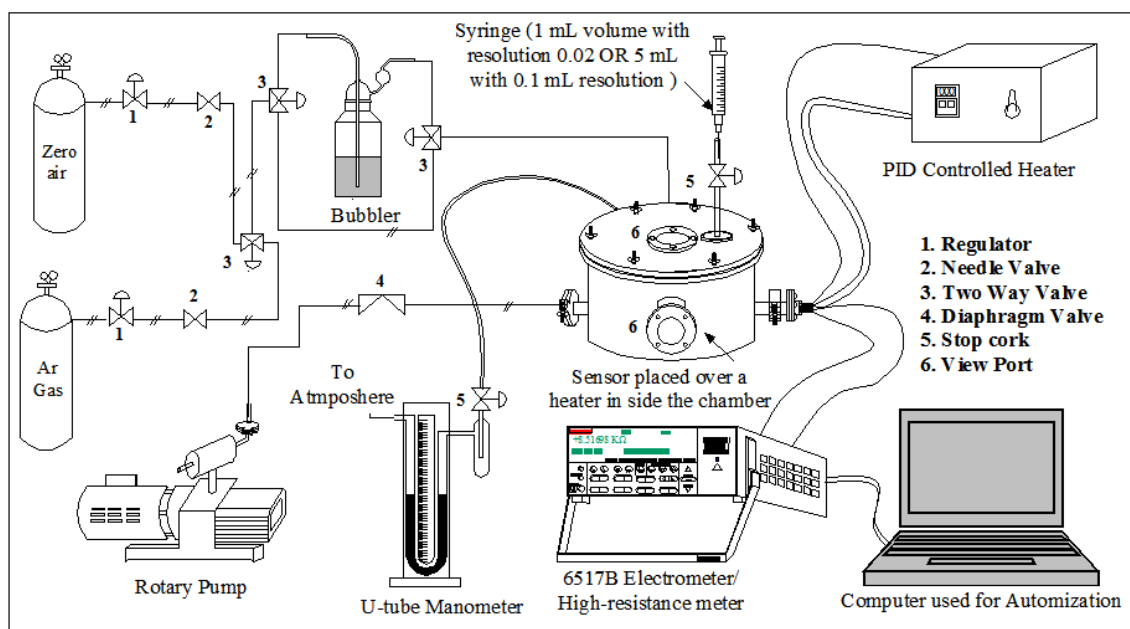


Figure 2. Schematic diagram of the in-house designed experimental set-up.

The sensor is heated at  $200^{\circ}\text{C}$  and subsequently degased using rotary pump. After this, the sample is maintained at the operating temperature that needs to be tested and the zero-air (air with moisture  $\leq 5$  ppm) is admitted to the chamber in order to create atmospheric pressure. The volume for the corresponding ppm concentration of alcohols is calculated using the following equation [16];

$$C \text{ (ppm)} = [10 C_1 V_1 dRT]/[P_0 V_c M] \quad (1)$$

where  $C_1$  is concentration in the liquid analyte (wt. %),  $V_1$  is the injected volume of liquid (ml),  $d$  is the density of the analyte (gm/ml),  $R$  is the universal gas constant (l.atm / K.mol),  $T$  is the temperature (K),  $P_0$  is the pressure in the chamber (atm),  $V_c$  is the chamber volume (l) and  $M$  is the molecular weight (gm / mol), respectively.

As some of the values in the equation-1 are constant, the concentration of analyte at room temperature (298 K) can be given as -

$$C \text{ (ppm)} = [C_1 V_1 d \times 244.66] / [P_0 V_c M] \quad (2)$$

$$V_1 \text{ (mL)} = [P_0 V_c M C] / [C_1 V_1 d \times 244.66] \quad (3)$$

For our case, the volume of the chamber,  $V_c = 1.35$  liter and the pressure maintained in the chamber,  $P_0 = 1$  atm.

The entire static-sensing studies carried out for both methanol and ethanol separately, consist of two parts. In the first part, the sensing behavior of the films are studied for the sensitivity of fixed concentrations of alcohols by temperature modulation to find the optimum sensing temperature ( $T_{opt}$ ), whereas in the second part, the alcohol sensitivity for different concentrations is studied at  $T_{opt}$ . In the present work, the alcohol analytes are Methanol (AR.99.9%, Sisco Research Laboratories Pvt. Ltd., India) and ethanol (AR.99.9%, Changshu Yangyuan Chemicals, China). The details of these experimental results are discussed in the following section.

### III. RESULTS AND DISCUSSION

#### 3.1. Characterization of sensing film

The XRD analysis is primarily used to confirm the sensing film material and to determine the structural orientation of sputtered-CuO film. Fig. 3 show XRD spectrum of annealed (550 °C, 2 h) as-deposited CuO sensing film. Although the background diffraction peaks of Si (100) substrate exist, three major diffraction peaks of  $Cu_xO_y$  are observed. These observed peaks with  $2\theta$  values of 28.1°, 35.6° and 47.7° corresponds to  $Cu_{16}O_{14.15}$  (112), CuO (002/-111) and  $Cu_{16}O_{14.15}$  (301) respectively. The CuO peak gives the highest intensity among them. Using Scherrer formula [17–18] grain size is calculated to be in the range of 52 nm.

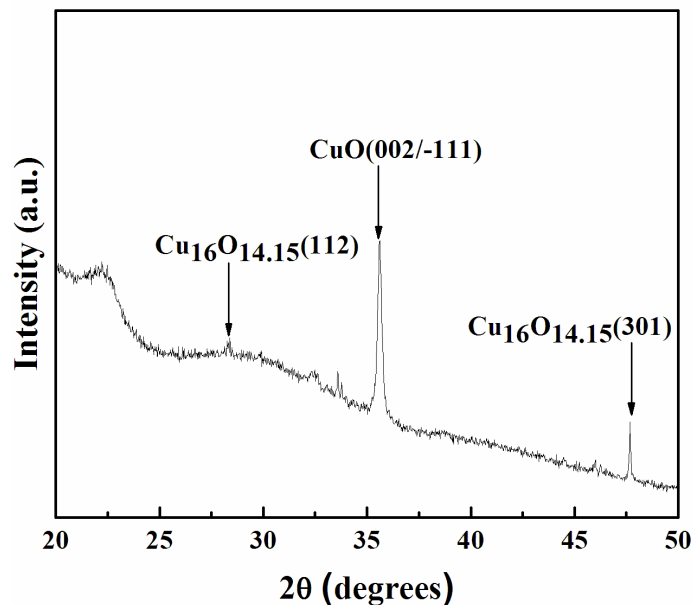


Figure 3. X-ray diffraction spectrum of annealed (550 °C, 2 h) as-deposited CuO sensing film.

The sensing film is analyzed using XPS in order to verify the stoichiometry of the film. Fig. 4(a)-(b) shows the spectra for copper and oxygen in CuO film. The peak for Cu ( $2P_{3/2}$ ) at binding energy of 933.88 eV showed the resemblance with the observation reported by Fleisch *et al.* [19] and McIntyre *et al.* [20]. Also, O (1S) peak at binding energy of 529.99 eV shows the resemblance with the results of Hirokawa *et al.* [21].

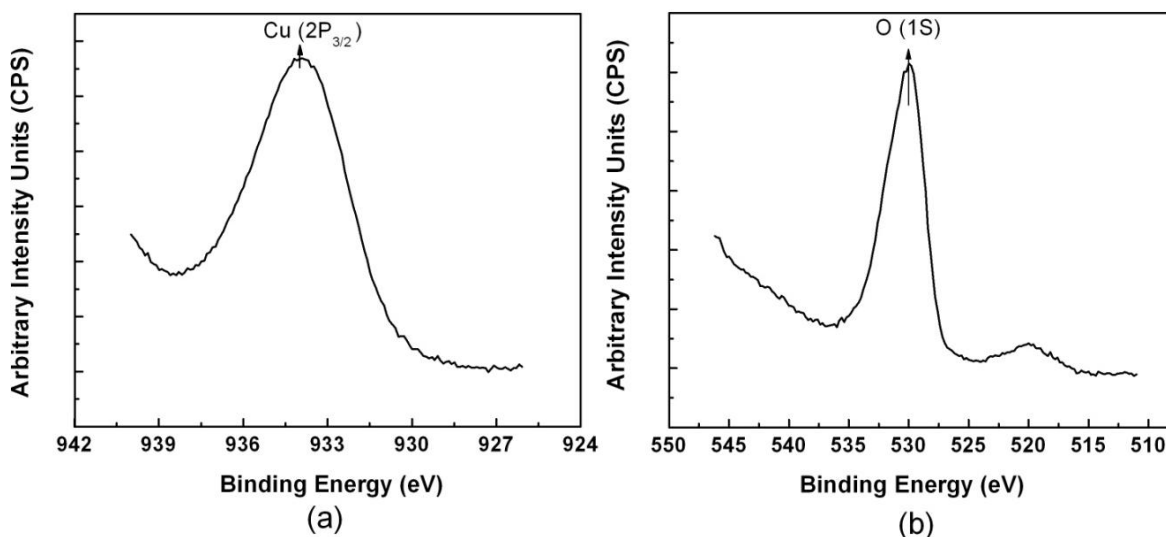


Figure 4. Core level XPS spectra of as-deposited CuO film (a) Cu  $2p_{3/2}$  and (b) O1s.

The SEM image of the as-deposited CuO film is shown in Fig. 5. When the grain size during FESEM imaging is measured, the film consists of nanostructures with size distribution of 40-65 nm. This size distribution can be attributed to high substrate temperature during the deposition of film. As small size of nanostructures increases surface area to volume ratio, the reactivity of the material increases, which in turn, will enhance the sensitivity of the sensing film. In addition to this, the grain boundaries between these nanostructures provide the resistance barrier for the charge carriers, hence increases the resistance of the film.

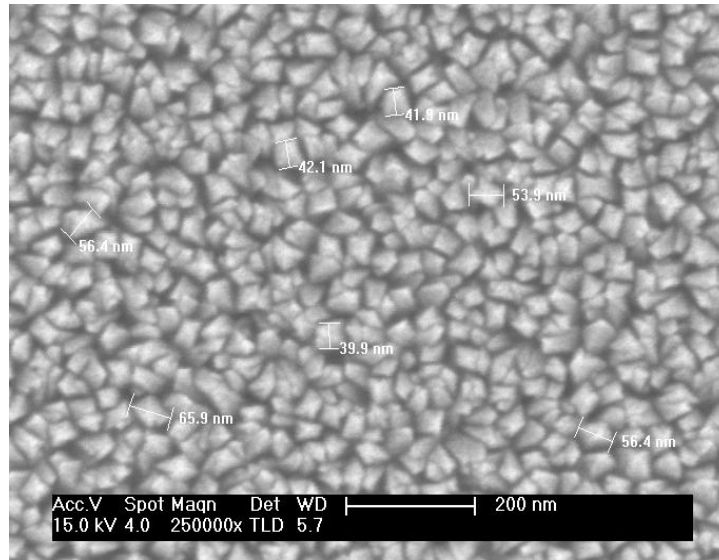


Figure 5. FESEM image of the as-deposited CuO film.

### 3.2. Response of sensing film for Methanol and Ethanol

As discussed above, the sensing film is kept at 200 °C in a closed chamber and degased using rotary pump. In order to create atmospheric pressure inside the chamber the zero-air is admitted in the chamber. Consequently, it has been observed that since CuO is a p-type semi-conducting material its resistance decreases and tends to be constant in approximately 3 minutes. The film resistance at that point of time is taken as initial/base resistance ( $R_{\text{air}}$  – resistance in the presence of air). Subsequently, when certain concentration of an methanol/ethanol is introduced in to the chamber, it is chemisorbed on the surface of the CuO film. Using pre-adsorbed oxygen atom, ethanol undergoes dehydrogenation in order to breakdown  $\text{CO}_2$  and  $\text{H}_2$ . During this dehydrogenation, it releases electrons into the film thereby increasing the number of minority charge carriers and reducing majority charge carriers in the p-type semiconducting film. This in turn, increases the resistance of the sensing film. The change in the film resistance saturates at

some point of time ( $R_g$  – resistance after the admittance of gas/analyte) depends upon the factors such as operating temperature, sensing material, active sensing area, concentration of the analyte, contact electrode patterns, etc. The sensitivity was calculated using the expression given in the literature [22]:

$$\text{Sensitivity} = [(R_{\text{gas}} - R_{\text{air}})/R_{\text{air}}] \times 100\% \quad (4)$$

One of the important things to consider here is the effect of operating temperature on the nanostructured sensing film. Once the sensor is tested at maximum operating temperature (450 °C) the film morphology tends to vary due to agglomeration. This leads to variation in the sensing response when measured again at lower temperature. In order to nullify the effect of varying operating temperature during the sensing, the film is annealed at 550 °C (i.e. maximum operating temperature (450 °C) + 100 °C) for 2 h.

### 3.2.1. Variation in the base resistance of the sensor as a function of operating temperature

The sensing response is measured using the electrometer, at fixed bias voltage of 10 V. As shown in Fig. 6, the film base resistance measured during the ethanol (500 ppm) sensing at varying operating temperature is observed to be 227 K $\Omega$  at 100 °C and subsequently decreased to 300  $\Omega$  at 500 °C. The base resistance measured during the methanol (500 ppm) sensing is almost equivalent to the base resistance values during ethanol sensing.

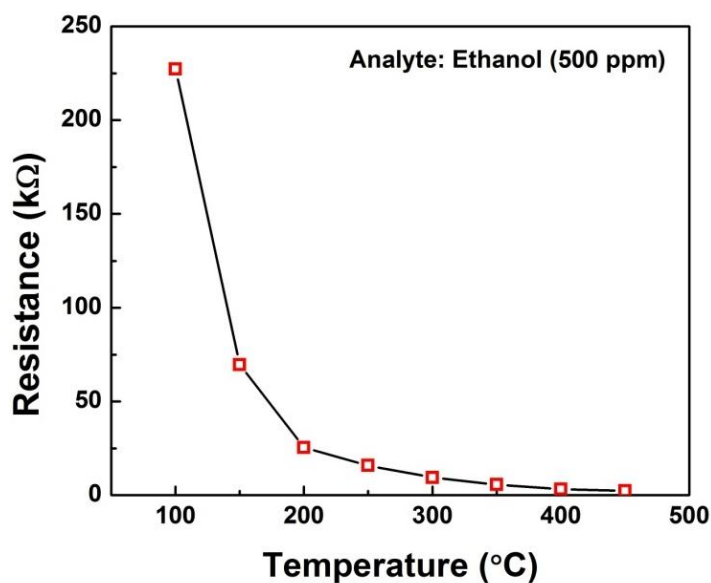


Figure 6. Variation in the base resistance of the sensing film with operating temperature modulation.

### 3.2.2. Optimization of the operating temperature for methanol and ethanol sensing

The sensitivity variation for methanol and ethanol with temperature modulation has been shown in fig. 7 (a) and (b). It may be noted that these temperatures 350 °C and 400 °C are the optimized operating temperatures ( $T_{opt}$ ) for methanol and ethanol respectively, where the sensitivity is the maximum. In order to confirm the repeatability of the results, the sensitivity is observed at different concentrations of 300-500-700 ppm for both the analytes for at least 3-5 times. The maximum sensitivity for 700 ppm of methanol and ethanol (separately) is observed to be 17% and 8.3% respectively. In the case of two-end electrode configuration the possibility of detection of induced charge carrier is quite low and the chances of recombination are high due to large inter-electrode distance (6 mm in present case) and mobility of charge carriers in CuO. The results obtained in the case of methanol and ethanol sensing, further validates the results reported by Cordi *et al.* [23]. According to their observation, the dehydrogenation of CH<sub>3</sub>OH/C<sub>2</sub>H<sub>5</sub>OH results in the formation of H/H<sub>2</sub>O and CO/CO<sub>2</sub>. In our case, the formation of CO<sub>2</sub> during the dehydrogenation indicates the complete breakdown of the ethanol. CO formed during this process may get converted into CO<sub>2</sub> using one oxygen atom. This oxygen atom might be pre-adsorbed over the sensing surface or can be from the CuO lattice. This results in partial reduction of CuO film into Cu<sup>+</sup> film varying the stoichiometry of the film. The major advantage of methanol/ethanol sensing from 350–400 °C is the oxidation of reduced sensing film which facilitates the easy recovery of the CuO sensing material [10, 24, 25]. This will help to maintain the stoichiometry. This will ultimately improve the reliability and shelf-life of the sensor. Moreover, sensing at very high temperature has advantage of nullifying the moisture effect.

The observed lower  $T_{opt}$  in the case of methanol compared to ethanol is believed to be due to its higher vapor pressure and thus lower energy is required to undergo complete dehydrogenation. Fig. 7 – (c) and (d) shows the resistance change during methanol and ethanol sensing at their  $T_{opt}$ , respectively. During complete sensor testing procedure, the base resistance varies  $\leq 1\%$ . This indicates that the sensing process is reversible with steady base resistance value.

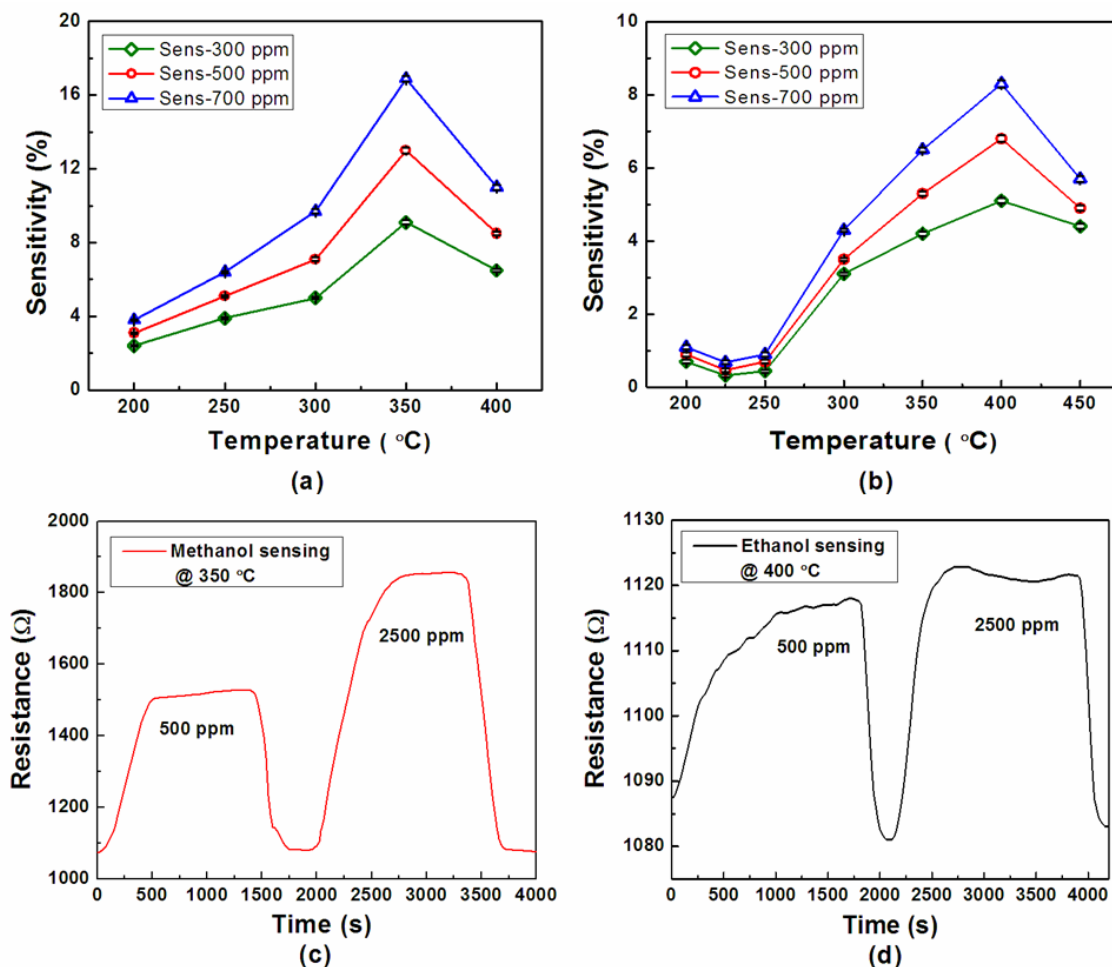


Figure 7. Sensitivity versus temperature graph of the CuO film for (a) methanol and (b) ethanol, respectively. (c–d) Resistance change during methanol and ethanol at respective  $T_{opt}$ .

### 3.2.3. Sensitivity with varying analyte concentrations

In order to study the sensor behavior by varying concentrations of methanol and ethanol, the sensitivity is further observed by concentration modulations (100 ppm to 2500 ppm) by maintaining their respective  $T_{opt}$  (Fig. 8). The figure also contains in-set graph showing the magnified version of the variation of the sensitivity versus analyte concentrations (with step-size of 100 ppm) for the concentration range 100 – 900 ppm. Although the sensitivity is linear for lower concentrations (for 100 to 900 ppm), it indicates a tendency of sensitivity saturation at higher concentrations (2500 ppm). The maximum sensitivity observed for 2500 ppm of methanol and ethanol is 29% and 15.4% respectively, and the maximum error-bar size is 0.25% and 0.16% of full scale for methanol and ethanol. The possible reason for this behavior might be the fixed/limited availability of active sensing area. When the analyte concentrations are low ( $\leq 900$

ppm), the proper sensing is possible as analyte molecules will form a monolayer over sensing film in order to be chemisorbed. This results into their complete chemisorption. On the contrary at higher concentrations ( $\approx 2500$  ppm), the analyte molecules left-over after the monolayer formation will not reach the sensing film in order to be chemisorbed. Hence, the chemisorption rate is limited due to limited active sensing area which in turn affects the sensitivity. The similar trends have been observed during both the analytes.

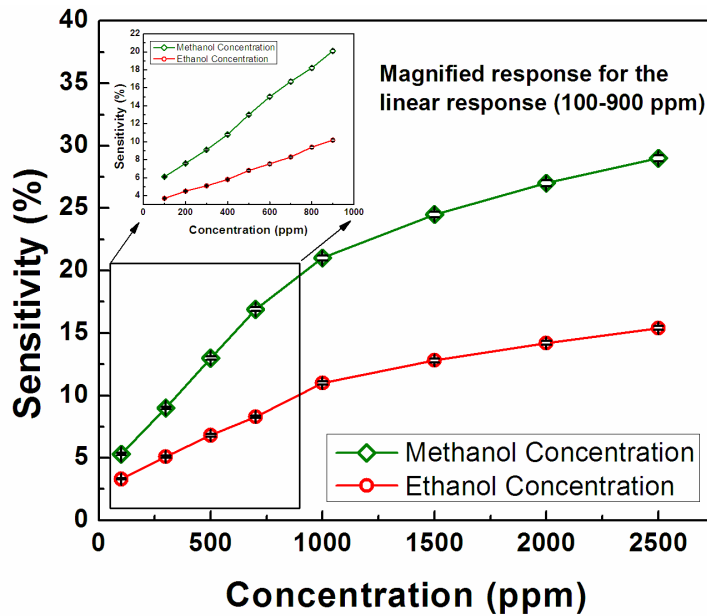


Figure 8. Sensitivity versus Methanol concentration and ethanol concentration at the operating temperature of  $350\text{ }^{\circ}\text{C}$  and  $400\text{ }^{\circ}\text{C}$  respectively.

#### 3.2.4. Response time and recovery time as a function of analyte concentrations

In addition to the above, the other important observation is regarding the response time and recovery time of the sensing film. The response time is the duration by which the sensor response reaches to almost 90% of the saturation value, whereas the recovery time is the duration by which the sensor response reaches from 90% to almost 10% of the saturation value. The sensing response time and recovery time depends upon the operating temperature of the sensor, the analyte type and their concentrations. Fig. 9(a-b) shows the effect of analyte type and varying concentrations of analyte on the response time and recovery time at the optimum operating temperatures of the analytes ( $350\text{ }^{\circ}\text{C}$  for methanol and  $400\text{ }^{\circ}\text{C}$  for ethanol).

From fig.9(a), it is evident that the sensing response time depends on the type of analytes and the analyte concentration. The response time of 2500 ppm methanol and ethanol is 235 s and 247 s correspondingly, and the maximum size of error-bar is of 18 s. The higher response time

for ethanol can be due to higher molecular weight of ethanol as compared to methanol, and hence, takes longer time to undergo dehydrogenation. In the case of varying concentration, the sensing response time is proportional to the analyte concentration, and tends to saturates at higher concentrations ( $\approx 2500$  ppm). This can be attributed to the limited/fixed active sensing area compared to the analyte concentration, hence lower rate of chemisorption or/and higher probability of inter-molecular collision of the analyte.

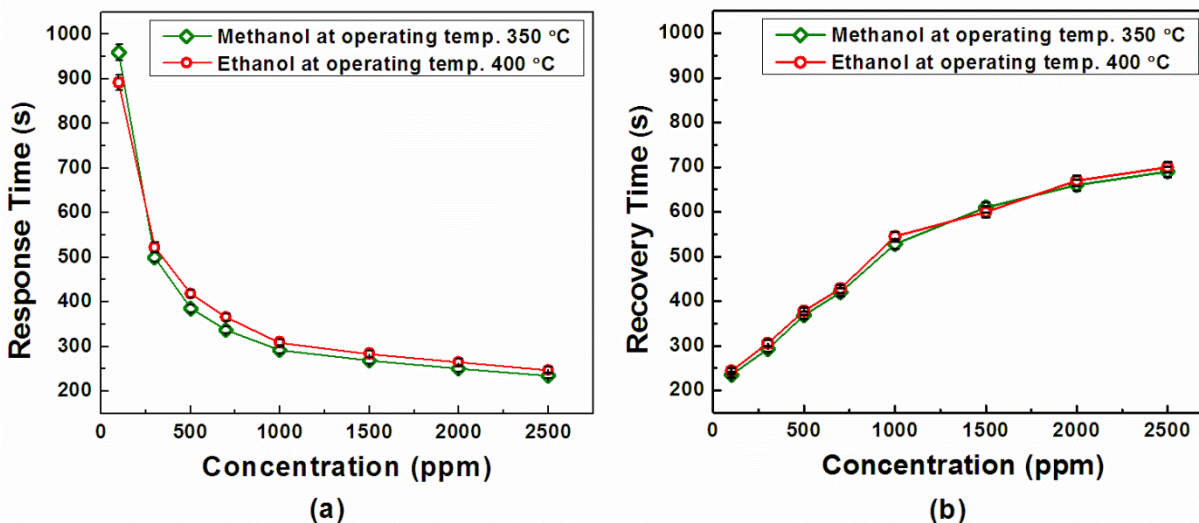


Figure 9. Effect of analyte concentration modulation on sensing response time and recovery time (a) methanol and (b) ethanol.

Fig.9(b) shows the dependency of recovery time on analyte concentration. The recovery time for both the analytes seems to be linear during lower concentrations ( $\leq 900$  ppm) and tends to saturates at higher concentrations ( $\geq 1000$  ppm). The recovery time for 100 ppm methanol and ethanol is 235 s and 244 s respectively, and the maximum error-bar size is found to be 12 s for 2500 ppm of both the analytes. When the analyte concentrations are low ( $\leq 900$  ppm), analyte molecules will form incomplete/complete monolayer over sensing film in order to be chemisorbed. Due to this chemisorption, the recovery time for the sensor increases linearly with lower concentration. On the contrary at higher concentrations ( $\approx 2500$  ppm), the analyte molecules left-over after the complete monolayer formation will not reach the sensing film in order to be chemisorbed. Hence, the recovery time tends to saturates at higher concentration. The similar trends have been observed during both the analytes.

#### IV. CONCLUSIONS

On the basis of the experimental techniques and the discussion of results in this paper, the possible applicability of nanostructured copper (II) oxide films for the methanol and ethanol sensing have been demonstrated. The optimum operating temperature for sensing of methanol and ethanol in the case of the CuO film is found to be 350 °C and 400 °C respectively, providing better sensitivity and selectivity. The sensitivity is found to be linear for lower concentrations and tends to saturate at higher concentrations. In addition to this, it has been concluded that the sensing response time also depend on the analyte concentration. This performance study on the CuO film will be helpful for the optimization of various important parameters, such as operating temperature and response time, leads to full-fledged methanol/ethanol sensor using nanostructured CuO as sensing film and might lead to whole new range of sensors using p-type semiconducting sensing material.

#### ACKNOWLEDGMENT

Authors wish to thank the Institute Nanoscience Initiative and the Central XRD facility at the institute campus for their kind help. Thanks are also to the Plasma processing lab at our department for XPS facility.

#### REFERENCES

- [1] W. Brattain and J. Bardeen, "Surface properties of Germanium", *Bell Syst. Tech. J.*, Vol. 32, 1953, pp. 1–41.
- [2] G. Heiland, "Zum Einfluss von adsorbiertem Sauerstoff auf die elektrische Leitfähigkeit von Zn-O-Kristallen", *Z. Physik*, Vol. 138, 1954, pp. 459–464.
- [3] A. Bielanski, J. Derren and J.Haber, "Electric conductivity and catalytic activity of semiconducting oxide catalysts", *Nature*, Vol. 179, 1957, pp. 668–669.
- [4] T. Seiyama, A. Kato, K. Fujiishi and M. Nagatani, "A new detector for gaseous components using semiconducting thin films", *Anal. Chem.*, Vol. 34, 1962, pp. 1502–1503.
- [5] G. Korotcenkov, "Metal oxides for solid-state gas sensors: What determines our

- choice?”, *Mater. Sci. Eng. B*, Vol. 139, 2007, pp. 1–23.
- [6] A. Chowdhuri, V. Gupta and K. Sreenivas, “Fast response H<sub>2</sub>S gas sensing characteristics with ultra-thin CuO islands on sputtered SnO<sub>2</sub>”, *Sens. Actuators B*, Vol. 93, 2003, pp. 572–579.
- [7] X. Zhou, Q. Cao, H. Huang, P. Yang and Y. Hu, “Study on sensing mechanism of CuO–SnO<sub>2</sub> gas sensors”, *Mater. Sci. Eng. B*, Vol. 99, 2003, pp. 44–47.
- [8] S. T. Jun and G. M. Choi, “CO gas-sensing properties of ZnO/CuO contact ceramics”, *Sens. Actuators B*, 17, Vol. 1994, pp. 175–178.
- [9] K. K. Baek and H. L. Tuller, “Atmosphere sensitive CuO/ZnO junctions”, *Solid State Ionics*, Vol. 75, 1995, pp. 179–186.
- [10] C. Wang, X.Q. Fu, X. Y. Xue, Y. G. Wang and T. H. Wang, “Surface accumulation conduction controlled sensing characteristic of p-type CuO nanorods induced by oxygen adsorption”, *Nanotechnology*, Vol. 18, 2007, pp. 145506–14510.
- [11] J. Bardeen, W. H. Brattain and W. Shockley, “Investigation of Oxidation of Copper by Use of Radioactive Cu Tracer”, *J. Chem. Phys.*, Vol. 14, 1946, pp. 714.
- [12] P. T. Moseley, “Solid state gas sensor”, *Meas. Sci. Technol.*, Vol. 8, 1997, pp. 223–237.
- [13] M. J. Madou and S. R. Morrison, “Chemical Sensing with Solid State Devices”, Academic Press, Inc./Harcourt Brace Jovanovich Publ., Boston, NY, 1987.
- [14] T. Ishihara, M. Higuchi, T. Takagi, M. Ito, H. Nishiguchi and Y. Takita, “Preparation of CuO thin films on porous BaTiO<sub>3</sub> and application as a CO<sub>2</sub> sensor”, *J. Mater. Chem.*, Vol. 8(9) 1998, pp. 2037–2042.
- [15] M. Parmar, N. Gokhale and K. Rajanna, “Nanostructured Copper(II) oxide thin film for alcohol sensing”, *Proceedings of IEEE International Instrumentation Measurement Technology Conference (I<sup>2</sup>MTC)– 2009* pp. 337–340.
- [16] T. Nakamoto, M. Yoshioka, Y. Tanaka, K. Kobayashi, T. Moriizumi, S. Ueyama and W. S. Yerazunis, “Colorimetric method for odor discrimination using dye-coated plate and multiLED sensor”, *Sens. Actuators B*, Vol. 116, 2006, pp. 202–206.
- [17] P. Scherrer, “Nachrichten von der Gesellschaft der Wissenschaften zu Göttingen”, 1918, pp. 98–100.
- [18] A. Patterson, “The Scherrer formula for X-Ray particle size determination”, *Phys. Rev.*, Vol. 56, 1939, pp. 978–982.

- [19] T. H. Fleisch and G. J. Mains, "Reduction of copper oxides by ultraviolet radiation and atomic hydrogen studied by XPS", *Appl. Surface Sci.*, Vol. 10, 1982, pp. 51–62.
- [20] N. S. McIntyre and M. g. Cook, "X-ray photoelectron studies on some oxides and hydroxides of cobalt, nickel and copper", *Anal. Chem.*, Vol. 47, No. 13, 1975, pp. 2208–2213.
- [21] K. Hirokawa, F. H. Honda and S. M. Oku, "On the surface chemical reactions of metal and oxide XPS samples at 300–400° at a high vacuum produced by oil diffusion pumps", *J. Electron Spectrosc.*, Vol. 6, 1975, pp. 333–345.
- [22] N.S. Ramgir, S. Kailasa Ganapathi, M. Kaur, N. Datta, K. P. Muthe, D. K. Aswal, S. K. Gupta and J. V. Yakhmi, Sub-ppm H<sub>2</sub>S sensing at room temperature using CuO thin films, *Sens. Actuators B*, Vol. 151, 2010, pp. 90–96.
- [23] E. M. Cordi, P. J. O'Neill and J. L. Falconer, "Transient oxidation of volatile organic compounds on a CuO/Al<sub>2</sub>O<sub>3</sub> catalyst", *Appl. Catal. B*, Vol. 14, 1997, pp. 23–36.
- [24] V. Figueiredo, E. Elangovan, G. Concalves, P. Barquinha, L. Pereira, N. Franco, E. Alves, R. Martins, and E. Fortunato, "Effect of post-annealing on the properties of copper oxide thin films obtained from the oxidation of evaporated metallic copper", *Applied Surface Science*, Vol. 254, 2008, pp. 3949-3954.
- [25] L. Zhou, S.Günther, D. Moszynski, and R. Imbihl, "Reactivity of oxidized copper surfaces in methanol oxidation", *J. Catalysis*, Vol. 235, No. 2, 2005, pp. 359–367.